

Construction of a miRNA-based prediction model for the prognosis of gastric cancer

Hanjue Dai^{1#}, Rui Ling^{1#}, Ya Xue¹, Yuan Qi¹, Fangfang Wu¹, Yunqian Chu¹, Qingying Xian¹, Jie Ding¹, Zhuxia Jia^{2*} and Wenyu Zhu^{1*}

¹ Department of Oncology, The Second People's Hospital of Changzhou, the Third Affiliated Hospital of Nanjing Medical University, Changzhou, 213003, China

² Department of Hematology, The Second People's Hospital of Changzhou, the Third Affiliated Hospital of Nanjing Medical University, Changzhou, 213003, China

Authors contributed equally: Hanjue Dai, Rui Ling

* Corresponding author, E-mail: jiazhuxia@163.com; wenyu.zhu@njmu.edu.cn

Abstract

Exosomal microRNAs (miRNAs) have emerged as promising biomarkers for gastric cancer (GC) prognosis. In this study, 76 GC patients treated at Changzhou Second People's Hospital (October 2020–May 2022) were prospectively enrolled, with monthly telephone follow-up to collect mortality and survival data for calculating overall survival. Exosomal miRNAs and clinical and pathological data from these patients constituted the training cohort, while validation was performed using a 400-patient cohort from The Cancer Genome Atlas database. A novel five-exosomal miRNA signature (miR-652-3p, miR-184, miR-340-3p, miR-96-5p, and miR-29a-3p) was identified as associated with overall survival. The resulting nomogram, which integrates this miRNA signature with key clinicopathological factors, achieved prognostic discrimination (C-index: 0.82). These findings demonstrate the clinical utility of this tool for individualized risk stratification.

Citation: Dai H, Ling R, Xue Y, Qi Y, Wu F, et al. 2025. Construction of a miRNA-based prediction model for the prognosis of gastric cancer. *Gastrointestinal Tumors* 12: e017 <https://doi.org/10.48130/git-0025-0016>

Introduction

Gastric cancer (GC) stands as a major and widely prevalent form of malignant neoplasm, posing a formidable threat to global public health^[1]. In 2022, statistical data revealed that the worldwide incidence of malignant tumors reached 19.965 million new cases, leading to 9.737 million deaths^[2]. GC, in particular, accounted for 968,000 of these new cases and 660,000 deaths, placing it fifth in both incidence and mortality rates^[2]. GC exhibits significant heterogeneity, with its pathogenesis comprising a complex interplay of multiple factors, gene regulation, and progressive stages^[3]. Consequently, the 5-year overall survival (OS) rate for GC patients remains low, and the overall mortality rate ranks third among cancer-related deaths^[1]. Thus, it is crucial to investigate the molecular markers linked to its prognosis, as well as to develop an efficient risk prediction model to enhance the OS rate of patients.

Recent advances in cancer diagnostics have utilized synthetic nanomaterials, such as DNA nanostructures and polymer-based sensors, for biomarker detection^[4]. Despite their programmable detection capabilities, these materials face significant clinical translation challenges: complex synthesis requiring specialized facilities, the immunogenicity risks from artificial components, and high production costs. In contrast, naturally derived exosomal microRNAs (miRNAs) offer inherent translational advantages. Their native human origin ensures biological compatibility by avoiding immune rejection. Standardized isolation uses US Food and Drug Administration (FDA)-approved protocols (e.g., ultracentrifugation), and detection via routine quantitative polymerase chain reaction (qPCR) aligns with cost-effective clinical workflows^[5].

miRNAs represent a class of endogenous noncoding RNAs, typically 22 nucleotides long, that are unable to encode proteins. However, they can bind to messenger RNAs through molecular sponging, thereby regulating gene expression at the post-transcriptional level^[6]. Studies have shown that miRNA is a key molecule

involved in the occurrence and development of GC, and can be a potential prognostic molecular marker for GC^[7].

Exosomes, with diameters ranging from 30 to 200 nm, are minuscule vesicles secreted by living cells and encased in lipid bilayer membranes^[8]. They are widely present in bodily fluids such as serum, urine, pleural effusion, and saliva. Exosomes contain various bioactive molecules including miRNA, long noncoding RNA, messenger RNA, proteins, and lipids^[8,9]. The formation and contents of extracellular vesicles are specific. The cellular components reflect both the phenotype and developmental origin of their parent cells. Exosomes play crucial roles in intercellular substance exchange and information transmission. Serving as "scouts" for tumor metastasis, exosomes participate in transmitting metastatic signals, promoting migration, inducing epithelial–mesenchymal transition, and creating a pre-metastatic niche. The abundance and stability of exosomal miRNAs make them significant in liquid biopsies. These miRNAs are internalized by the recipient cells through various mechanisms, exerting regulatory effects on the target genes within those cells^[10]. Thus, exosomal miRNAs hold potential as biological markers for the diagnosis and prognosis of GC.

Our research centered on isolating plasma from GC patients to sequence exosomal miRNAs. We then analyzed these miRNAs in conjunction with clinical features and prognostic information. Ultimately, we constructed a miRNA-based prediction model and confirmed its predictive efficacy using The Cancer Genome Atlas (TCGA) GC dataset. Our goal was to enhance the understanding of the relationship between exosomal miRNAs and the prognosis of GC.

Materials and methods

Study design and patients

This study was a single-center observational study. Approval for this study was obtained from the Ethics Committee of the

Changzhou Second People's hospital (approval number: [2020] KY261-01). We enrolled 76 GC patients who were treated at Changzhou Second People's hospital from October 2020 to May 2022, and all patients provided written informed consent. They were followed up once a month by telephone after discharge. Throughout the study period, data on mortality and survival rates were collected, allowing for calculation of the OS rate. The clinical and pathological data of the participants were collected as the training group.

Study participants had to meet the following criteria: (1) The diagnosis of GC was implemented according to the World Health Organization's (WHO's) pathological diagnostic criteria; (2) none of the patients had any additional immune, endocrine, or metabolic diseases; (3) the patients who had not undergone any antitumor treatment prior to admission; and (4) the patient did not receive antitumor treatment before the peripheral blood sample collection period.

GC data were obtained from TCGA database (<https://portal.gdc.cancer.gov>), and a cohort of 400 patients with comprehensive data encompassing survival time, survival status, cancer stage, gender, age, and miRNA profiles were selected. This dataset served as the validation group for our study.

Isolation of plasma exosomes

Extracellular vesicle (EV) extraction was performed using the ExoQuick-TM kit (SBI, USA) following the manufacturer's instructions. The extracted EV samples were stained and observed under an electron microscope to examine their particle morphology.

miRNAs sequencing and data analysis

Sequencing was performed using the Illumina Nextseq 500 platform (Illumina, USA). Subsequently, the raw sequencing data were analyzed for quantification of miRNA expression and miRNA differential expression analysis.

Statistical analysis

All analyses were performed using R 4.2.2 statistical software (www.r-project.org). Continuous variables are presented as the mean \pm standard deviation (SD) (normally distributed) or median (P25, P75) (non-normal), compared by Student's *t*-test or the Mann–Whitney U-test (Shapiro–Wilk normality test). Categorical variables are expressed as *n* (%) and were analyzed by Chi-square or Fisher's exact test. Qualitative data are presented as absolute numbers or percentages. The Kaplan–Meier method was used to plot survival curves and compute the OS rate, and the log-rank test was used to compare survival outcomes between the two groups. For multiple testing correction, miRNA *p*-values from the univariate analysis were adjusted by the Benjamini–Hochberg false discovery rate (FDR) (*q* < 0.05). Statistical significance was defined as two-sided *p* < 0.05 (or *q* < 0.05 for the FDR).

Least absolute shrinkage and selection operator–Cox dimension reduction analysis

We conducted a least absolute shrinkage and selection operator (LASSO)–Cox dimension reduction analysis using the 'glmnet' and 'survival' packages in R. The λ value that corresponded to the minimal partial likelihood deviance was chosen as the optimal λ for our study. Normalized read counts underwent \log_2 -transformation (training cohort only). Feature selection was performed via 10-fold cross-validated LASSO–Cox regression (maximum iterations = 1,000). The regularization parameter λ was determined at 1 standard error from the minimum partial likelihood deviance (optimal $\lambda = 0.15$). Post-selection criteria required miRNA detection in > 90% of the training samples. Multivariate Cox analysis confirmed

independent prognostic significance after adjustment for clinical covariates.

Risk score = $\text{expr}_{\text{miR-652-3p}} \times \lambda_{\text{miR-652-3p}} + \text{expr}_{\text{miR-184}} \times \lambda_{\text{miR-184}} + \text{expr}_{\text{miR-340-3p}} \times \lambda_{\text{miR-340-3p}} + \text{expr}_{\text{miR-96-5p}} \times \lambda_{\text{miR-96-5p}} + \text{expr}_{\text{miR-29a-3p}} \times \lambda_{\text{miR-29a-3p}}$ where $\text{expr}_{\text{miRNA}}$ represents the expression level of the miRNA, and λ_{miRNA} is the associated λ value.

Analysis of cell signaling pathways

The target genes of the five miRNAs used for GC prognosis were predicted using the miRPath v4.0 online analysis tool. Enrichment analysis of the cell signaling pathways was conducted, alongside Gene Ontology (GO) and Kyoto Encyclopedia of Genes and Genomes (KEGG) enrichment analysis of the target genes. The top 20 pathways were then visualized.

Construction of nomograms

A nomogram analysis was developed for the training group using the 'rms' package in R. The upper section of the nomogram represents the scoring system, while the lower section constitutes the prediction system. This tool accurately forecasts the 1-year, 2-year, and 3-year OS rates of the GC patients by calculating the total points (the sum of the points awarded for each factor). The prediction accuracy for OS was verified in the validation group. Calibration curves and the concordance index (C-index) values were used to demonstrate the precision of the survival predictions.

Results

Prevalence of GC patients

The training group comprised 76 GC patients, including 55 men and 21 women, with an average age of 67.34 ± 9.46 years. Forty-two cases died in the training group, accounting for 55.26% (Table 1). The validation group consisted of 400 GC patients, including 261 men and 139 women, with a mean age of 64.49 ± 11.85 years; 240 cases died in the validation group, accounting for 60% (Table 1). The training group had more advanced tumors (Stage IV/T4/M1, all *p* < 0.01). The validation cohort showed a higher N1 rate (*p* < 0.01). This reflects inherent selection biases: single-center studies often treat more aggressive cases, while the TCGA predominantly includes surgical candidates^[11].

Construction of miRNA risk score

Comprehensive miRNA profiling identified 1,334 distinct miRNAs in the training group and 2,158 in the validation group. Finally, we identified five candidate miRNAs along with their respective lambda values (miR-652-3p: -0.0529964688819932; miR-184: 0.00193748008867359; miR-340-3p: 0.0513602381783128; miR-96-5p: 0.0475860943623225; miR-29a-3p: 0.123147129022319) using LASSO–Cox, which were based on the OS of the GC patients in the training group (Fig. 1a, b).

The miRNA risk score equation constructed from these five miRNAs was Risk score = $\text{expr}_{\text{miR-652-3p}} \times -0.0529964688819932 + \text{expr}_{\text{miR-184}} \times 0.00193748008867359 + \text{expr}_{\text{miR-340-3p}} \times 0.0513602381783128 + \text{expr}_{\text{miR-96-5p}} \times 0.0475860943623225 + \text{expr}_{\text{miR-29a-3p}} \times 0.123147129022319$.

The coefficient sign and magnitude of each miRNA indicate its prognostic function: miR-652-3p acts as a protective factor (risk-reducing); miR-184 contributes minimally to risk; and miR-340-3p, miR-96-5p, and miR-29a-3p function as risk-increasing factors, of which miR-29a-3p is the primary risk driver because of its dominant coefficient magnitude.

The predefined multigene signature formula was applied to compute miRNA risk scores for both the training and validation

Table 1. Baseline characteristics of GC patients in the training and validation groups

Variables		Training group (n = 76)	Validation group (n = 400)	p-value
Age (years)		67.34 ± 9.46	64.49 ± 11.85	0.05
Time (days)		1,095.00 (431.00, 1,095.00)	460.00 (274.75, 782.75)	< 0.01
Status	Dead	42 (55.26%)	240 (60.00%)	0.44
	Alive	34 (44.74%)	160 (40.00%)	
Gender	Female	21 (27.63%)	139 (34.75%)	0.23
	Male	55 (72.37%)	261 (65.25%)	
Stage	I	17 (22.37%)	50 (12.50%)	< 0.01
	II	9 (11.84%)	130 (32.50%)	
	III	27 (35.53%)	181 (45.25%)	
	IV	23 (30.26%)	39 (9.75%)	
Tumor stage	1	12 (15.79%)	16 (4.00%)	< 0.01
	2	11 (14.47%)	82 (20.50%)	
	3	5 (6.58%)	188 (47.00%)	
	4	48 (63.16%)	114 (28.50%)	
Metastasis	0	53 (69.74%)	358 (89.50%)	< 0.01
	1	23 (30.26%)	26 (6.50%)	
	Unknown	0 (0.00%)	16 (4.00%)	
Spread of cancer to lymph nodes	0	26 (34.21%)	125 (31.25%)	< 0.01
	1	7 (9.21%)	105 (26.25%)	
	2	18 (23.68%)	81 (20.25%)	
	3	25 (32.89%)	84 (21.00%)	
	Unknown	0 (0.00%)	5 (1.25%)	
Lauren classification	Intestinal	42 (55.26%)	83 (56.08%)	0.12
	Diffuse	29 (38.16%)	63 (42.57%)	
	Mixed	5 (6.58%)	2 (1.35%)	
Radiotherapy	Not performed	57 (75.00%)	296 (79.36%)	0.40
	Performed	19 (25.00%)	77 (20.64%)	
Pharmaceutical therapy	Not performed	31 (40.79%)	188 (50.40%)	0.13
	Performed	45 (59.21%)	185 (49.60%)	

cohorts. Patients were stratified into high-risk (score > median) and low-risk (score ≤ median) groups using the cohort-specific median score as the threshold. Kaplan–Meier analysis compared the OS between these risk strata. The results showed that the OS rate of the

low-risk group was higher in the training dataset ($p < 0.0001$) and the validation dataset ($p = 0.021$) (Fig. 2a, b).

Functional analysis of prognosis-related miRNA target genes in GC patients

The target genes of the five miRNAs used for GC prognosis were predicted using the miRPath v4.0 online analysis tool. Enrichment analysis of the cell signaling pathways was conducted, alongside GO and KEGG enrichment analysis of the target genes. The top 20 pathways were then visualized. (Fig. 3a, b). The top 20 enriched terms of the KEGG enrichment analysis were shigellosis, focal adhesion, the P13K-Akt signaling pathway, the FoxO signaling pathway, prostate cancer, viral carcinogenesis, epidermal growth factor receptor (EGFR) tyrosine kinase inhibitor, resistance, proteoglycans in cancer, adherens junction, the p53 signaling pathway, regulation of the actin cytoskeleton, cell cycle, small-cell lung cancer, colorectal cancer, human papillomavirus infection, pathways in cancer, hepatocellular carcinoma, bacterial invasion of epithelial cells, apoptosis, and salmonella infection. The top 20 enriched terms of the GO enrichment analysis were protein binding, cytosol, nucleus, nucleoplasm, cytoplasm, RNA binding protein-containing complex, viral process, cadherin binding, chromatin organization, negative regulation of transcription by RNA polymerase II chromatin binding, DNA binding, extracellular exosome, transferase activity, positive regulation of transcription by RNA polymerase, focal adhesion, rhythmic process, positive regulation of transcription, DNA-template, and cytoplasmic stress granules.

Construction and evaluation of nomogram

A prognostic nomogram was developed by integrating the miRNA risk score with variables such as age, the tumor's pathological stage, risk score, radiotherapy, and pharmaceutical therapy (Fig. 4). To assess the accuracy of the nomogram in predicting the OS rate, a calibration curve was used. The 45° dotted line in the figure represents an ideal curve, suggesting that the predicted OS rate aligns closely with the actual survival outcomes. The figure illustrates that the 1-year, 2-year, and 3-year OS rates for GC patients, as predicted by the nomogram in both the training and validation dataset, are closely aligned with the actual OS rate (Fig. 5a, b). Additionally,

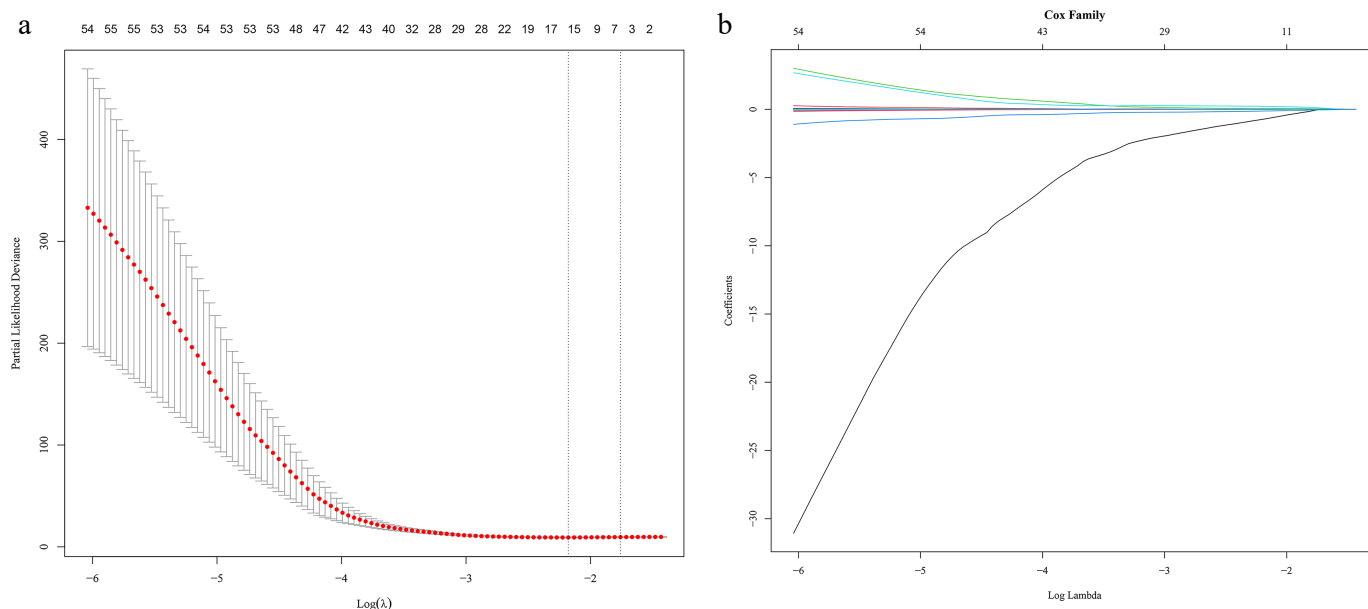


Fig. 1 (a) LASSO deviance profiles for miRNAs associated with GC patients in the training group. (b) LASSO coefficient profiles for miRNAs associated with GC patients in the training group.

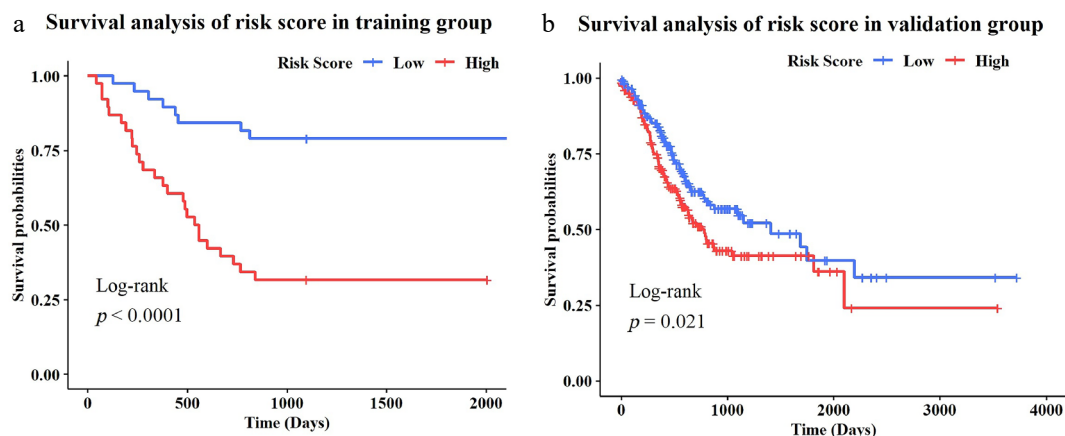


Fig. 2 (a) Survival curves of the effect of miRNA-based risk scores on GC patients in the training group. (b) Survival curves of the effect of miRNA-based risk scores on GC patients in the validation group.

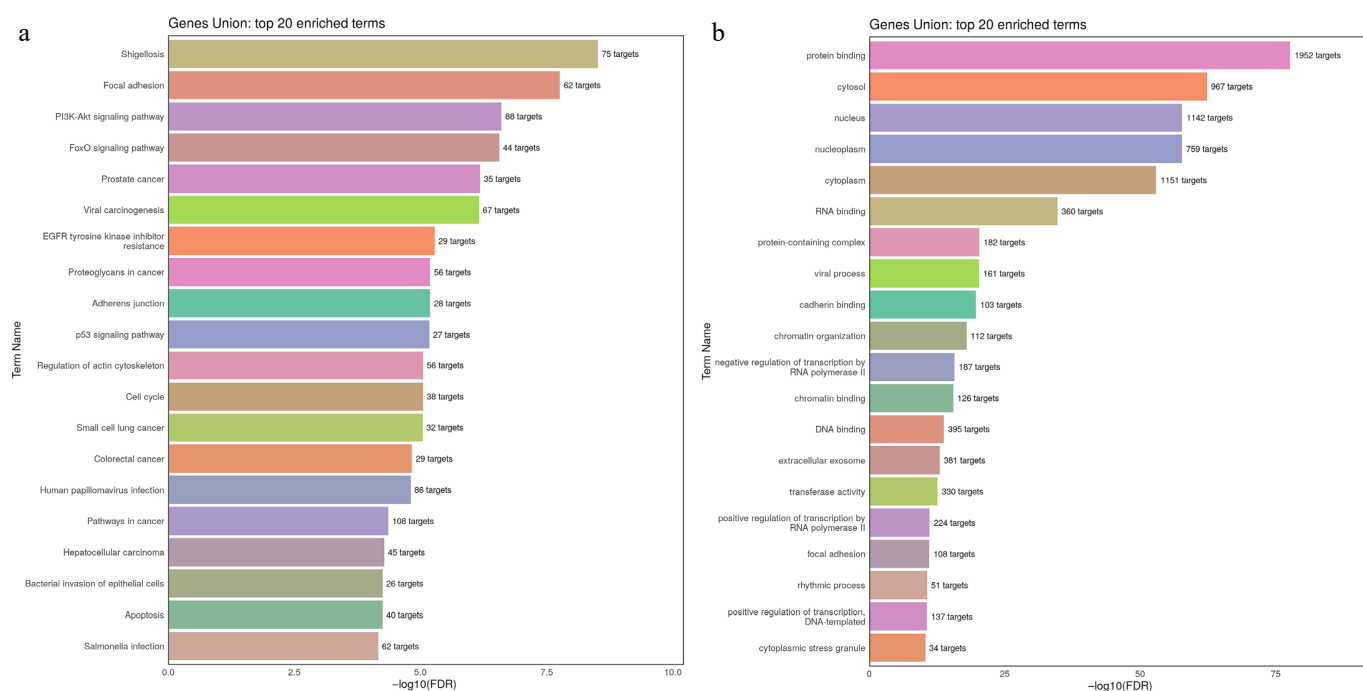


Fig. 3 (a) KEGG enrichment analysis of the miRNAs' target genes. (b) GO pathway enrichment analysis of the miRNAs' target genes.

the C-index for the nomogram, along with age, stage, risk score, radiotherapy, and pharmaceutical therapy, was calculated. Upon comparison, it was observed that the nomogram had the highest C-index, i.e., 0.82 (Fig. 6). Decision curve analysis (DCA) revealed that patients could gain significant benefits from use of the nomogram in clinical decision-making (Fig. 7).

Discussion

With the advance of high-throughput sequencing technology, the integrated analysis of multiple omics, including genomics, transcriptomics, and proteomics, has emerged as a prominent field in biological research^[12]. miRNA regulatory networks play critical roles in disease pathogenesis through post-transcriptional gene regulation. These small noncoding RNAs modulate the target genes' expression by inducing mRNA degradation or translational repression^[13]. Alterations in miRNA expression or dysfunction can significantly impact tumors' initiation and development. Researches have demonstrated that miRNA serves as a potential prognostic

factor for GC, participating in numerous processes such as the proliferation, differentiation, metastasis, and drug resistance of GC^[14]. For example, miR-6165 had been reported to be underexpressed in GC tissues and to regulate the upregulation of STRN4, thereby facilitating the migration and invasion of GC cells^[15]. Research indicates that N2 tumor-associated neutrophils (N2-TANs) convey miR-47445-5p and miR-3911 via their originating exosomes, and are capable of downregulating the expression of SLIT2 in GC cells, consequently facilitating the metastasis of GC^[16]. In addition, it has been discovered that miRNA arm-imbalance contributes to the progression of GC. Altering miR-574's targets may represent a promising therapeutic strategy for treating this disease^[17]. Our study aimed to detect the expression levels of circulating exosomal miRNAs in GC patients through high-throughput sequencing combined with bioinformatics methods. By using LASSO-Cox regression, we identified five miRNAs related to the prognosis of GC, namely miR-652-3p, miR-184, miR-340-3p, miR-96-5p and miR-29a-3p. Based on these miRNAs, a risk score was obtained. Finally, a nomogram model was constructed by combining age, the tumors'

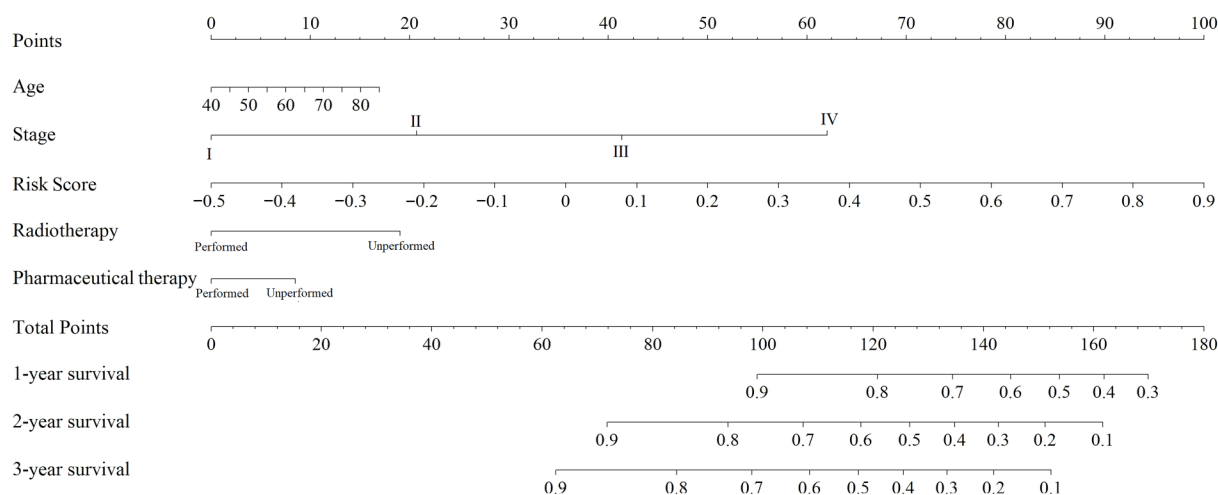


Fig. 4 Nomogram for predicting the survival rate of GC patients.

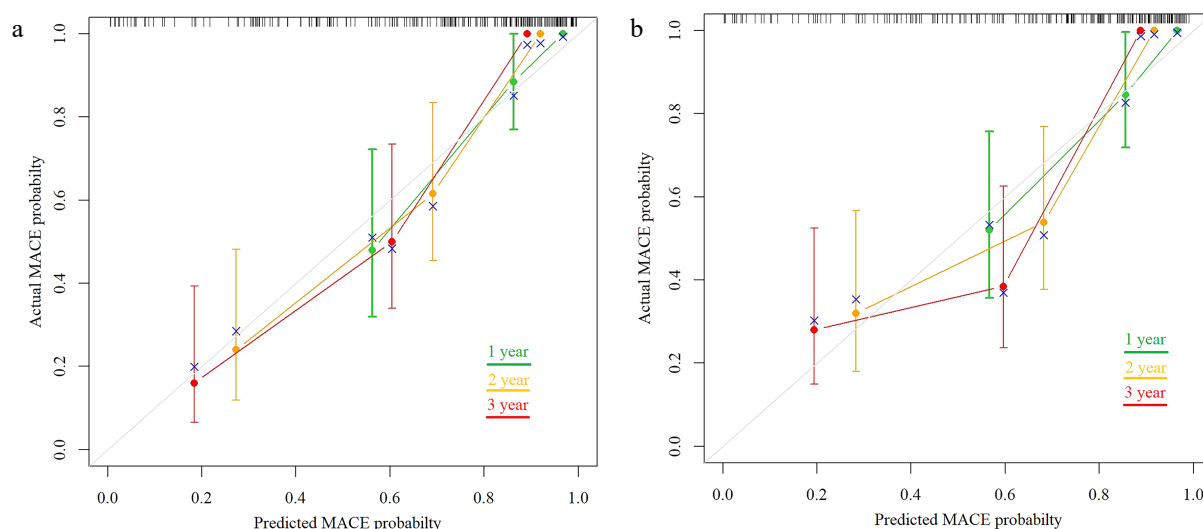


Fig. 5 (a) Calibration plot of the comparison between the predicted and actual survival probability over 1, 2, and 3 years in the training group. (b) Calibration plot of the comparison between predicted and actual survival probability over 1, 2, and 3 years in the validation group.

pathological stage, risk score, radiotherapy, and pharmaceutical therapy.

miR-652-3p demonstrates context-dependent duality in tumorigenesis, functioning as both a tumor suppressor and an oncogene across malignancies^[18]. This functional divergence may stem from tumor-specific microenvironments, distinct target gene repertoires, or unidentified molecular modifiers. Experimental validation of multiple miR-652-3p targets has confirmed its regulatory role in core oncogenic pathways^[18]. Dysregulation of miR-652-3p has been documented in gastrointestinal cancers, including esophageal, gastric, and colorectal carcinomas. RNA sequencing revealed significant upregulation in GC patients' serum^[19], corroborated by real-time qPCR in plasma samples from 50 GC patients. Notably, miR-652-3p (alongside miR-627-5p and miR-629-5p) shows promise as a noninvasive diagnostic and prognostic biomarker panel for GC^[20].

Dysregulation of miR-184 is consistently observed in human tumor specimens across multiple malignancies. Its expression levels correlate significantly with clinicopathological parameters, establishing miR-184 as a validated prognostic biomarker^[21,22]. Functional studies have demonstrated that exogenous miR-184 supplementation acts as a tumor suppressor, inhibiting neoplastic proliferation

and metastatic dissemination in both cell culture and animal models. These findings position miR-184 as a promising therapeutic target in oncology. The expression of miR-184 in GC tissues is related to lymph node metastasis and the tumor size-lymph node involvement-metastasis (TNM) stage, and the mechanism may be that the inhibition of miR-184 expression induces the activation of extracellular signal-regulated kinase 1, which increases the translation of its expression products, thereby shortening the cell cycle and accelerating the division and differentiation of cancer cells^[23]. Furthermore, downregulated miR-184 activates tumor necrosis factor- α , which, in turn, activates vascular endothelial growth factor and insulin-like growth factor 2, promoting the formation of tumor neovascularization around cancer cells and enhancing their metastasis and invasion capabilities^[24].

miR-340, an intragenic miRNA encoded within Intron 5 of the *RNF130* gene (chr5q35.3)^[25], demonstrates pan-cancer dysregulation with diagnostic biomarker potential. In GC, epigenetic silencing via CpG island hypermethylation in its promoter region correlates with pathogenesis^[26]. Notably, miR-340 shows significant overexpression in miRNA profiles of GC tissue^[27], suggesting its utility for detection and stratification of GC.

Mature miR-96-5p (derived from the miR-96 precursor at 7q32.2) exhibits oncogenic properties in breast cancer and thyroid cancer^[28]. In GC, miR-96-5p drives tumor progression by direct targeting of ZDHHC5 to enhance cell proliferation and invasion^[29]. These coordinated functions establish miR-96-5p as a candidate diagnostic biomarker and therapeutic target for GC^[30].

As a member of the miR-29 family, miR-29a-3p has been implicated in regulating the onset and progression of various cancers^[31]. It is involved in the pathogenesis of numerous tumors, such as influencing the drug resistance of cancer cells to chemotherapy by directly regulating the collagen Type V alpha 2 chain^[32,33]. In highly metastatic GC cell lines, miR-29a-3p expression is significantly downregulated. Functional restoration experiments demonstrate that miR-29a-3p overexpression suppresses oncogenic phenotypes—including proliferation, clonogenicity, migration, and invasion—establishing its therapeutic potential for metastatic GC^[34].

The interaction between miRNA and its target genes is intricate, potentially involving the regulation of multiple target genes by several miRNAs, thereby establishing a complex regulatory network^[35]. By integrating bioinformatics techniques with large-scale database analyses, the relationship between miRNA and the occurrence and progression of cancer, along with its potential signaling mechanisms, can be elucidated more systematically. KEGG pathway and GO functional enrichment analyses (performed using miRPath v4.0) suggested that the target genes of these miRNAs were significantly enriched in proliferation-associated pathways (e.g., the PI3K-AKT signaling pathway, cell cycle)^[36–38]. These findings imply a potential functional relevance in modulating the progression of GC; however, the precise biological roles of these exosomal miRNAs require experimental validation in future studies. The miRNA-based prediction model provides a tool for individualized risk assessment to inform patient counseling and surveillance strategies. This model also enables stratification of GC patients into distinct prognostic subgroups. For example, high-risk patients may be prioritized for more frequent follow-up or adjuvant therapy trials, whereas low-risk cohorts could avoid overtreatment.

The training cohort had a higher proportion of advanced-stage patients (Stage IV: 30.26% vs 9.75%) and distant metastases (M1: 30.26% vs 6.5%) compared with the TCGA validation cohort. This reflects inherent selection biases: single-center studies often treat more aggressive cases, while the TCGA predominantly includes surgical candidates^[11]. Crucially, the model maintained accuracy across these divergent populations, which underscores its robustness for broad clinical application.

However, this study has the following limitations. Firstly, the study is limited by a small sample size. It is necessary to collect large-scale,

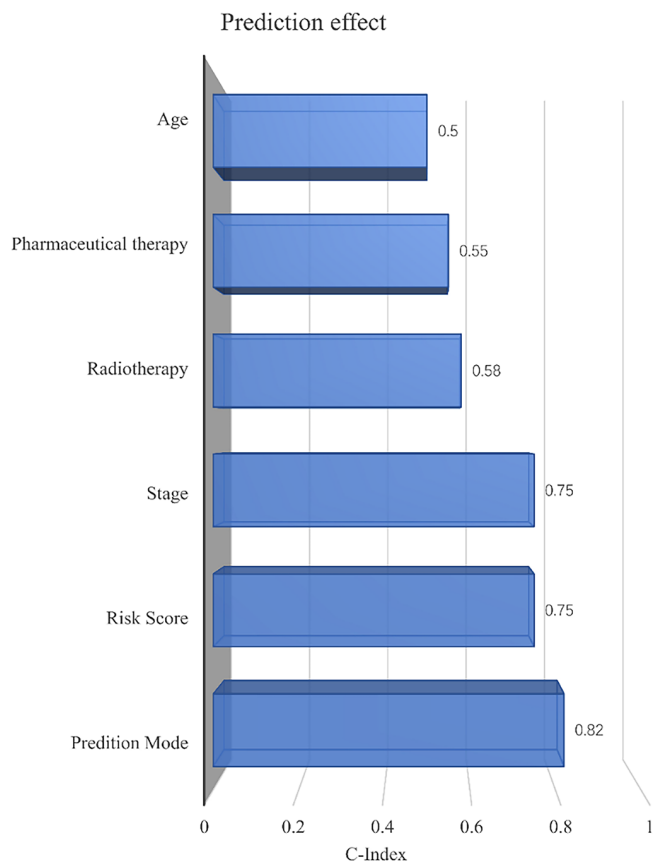


Fig. 6 The predictive effect of the nomogram model, risk score, age, radiotherapy, pharmaceutical therapy, and the tumor's pathological stage in GC patients on OS was evaluated by the C-index.

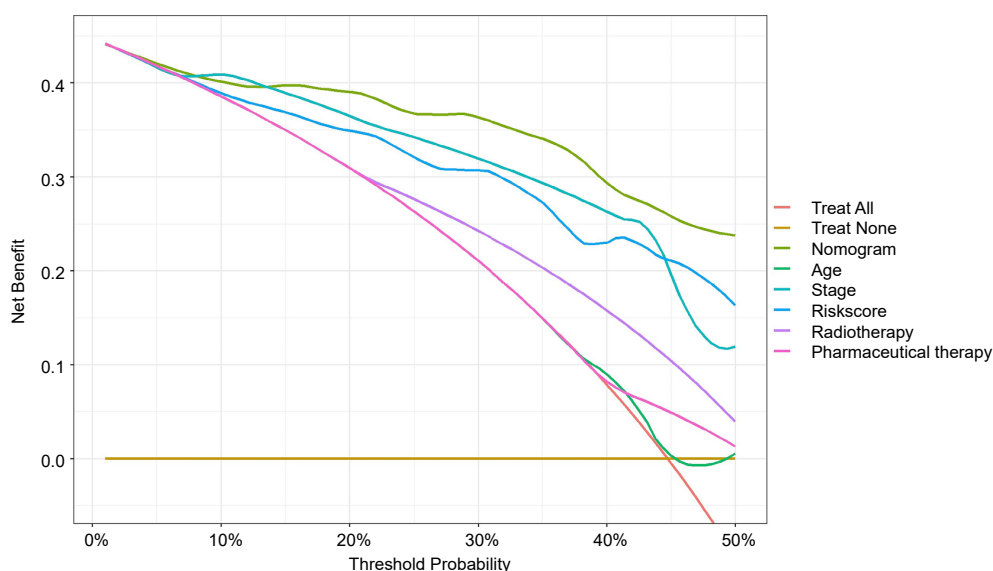


Fig. 7 DCA revealed that patients could gain significant benefits from use of the nomogram in clinical decision-making.

multi-center clinical data to further validate the efficacy of this model and to investigate the mechanisms of the five miRNAs through both *in vivo* and *in vitro* experiments. Moreover, the expression of miRNAs undergoes dynamic changes during different stages of tumor development and within varying microenvironments. In the early and late stages of GC, miRNA expression patterns may alter significantly. The model constructed here might not adequately adapt to these dynamic changes. The nomogram identifies high-risk patients who may benefit from intensified monitoring or enrollment in clinical trials, but it does not prescribe specific therapies. Treatment decisions should integrate this risk profile with established clinical guidelines and patient-specific factors. Finally, the expression of miRNA can be influenced by various factors, including diet, ethnicity, and environmental factors. Furthermore, the lack of standardization in miRNA detection techniques means that different methods used by different laboratories can result in inconsistent detection outcomes^[18]. These factors collectively impact the model's accuracy.

Conclusions

We developed a plasma exosomal miRNA-based signature (miR-652-3p, miR-184, miR-340-3p, miR-96-5p, and miR-29a-3p) and integrated it with clinicopathological factors to construct a prognostic nomogram. The model demonstrated robust performance in predicting GC outcomes and may aid risk stratification for personalized management. The biological significance of this signature warrants further investigation.

Ethical statements

The study protocol was performed in accordance with the ethical guidelines of the 1975 Declaration of Helsinki. Approval for this study was obtained from the Ethics Committee of the Changzhou Second People's hospital (approval number: [2020]KY261-01). Moreover, written informed consent was obtained from the patients for publication of this study.

Author contributions

The authors confirm contribution to the paper as follows: study conception and design: Dai H, Ling R, Jia Z, Zhu W; data collection: Xue Y, Qi Y; analysis and interpretation of results: Wu F, Chu Y, Xian Q, Ding J; draft manuscript preparation: Dai H. All authors reviewed the results and approved the final version of the manuscript.

Data availability

The datasets generated during and/or analyzed during the current study are available from the corresponding author on reasonable request.

Acknowledgments

The authors gratefully acknowledge the research members and participants in this study, without whom it would not have been possible. This study was supported by Changzhou Sci&Tech Program to C.Y. (Grant No. CJ20243018) and to Z.W. (Grant No.CJ20243019).

Conflict of interest

The authors declare that they have no conflict of interest.

Dates

Received 10 February 2025; Revised 20 July 2025; Accepted 22 August 2025; Published online 29 October 2025

References

1. Arnold M, Park JY, Camargo MC, Lunet N, Forman D, et al. 2020. Is gastric cancer becoming a rare disease? A global assessment of predicted incidence trends to 2035. *Gut* 69:823–29
2. Bray F, Laversanne M, Sung H, Ferlay J, Siegel RL, et al. 2024. Global cancer statistics 2022: GLOBOCAN estimates of incidence and mortality worldwide for 36 cancers in 185 countries. *CA: A Cancer Journal for Clinicians* 74:229–63
3. Smyth EC, Nilsson M, Grabsch HI, van Grieken NC, Lordick F. 2020. Gastric cancer. *The Lancet* 396:635–48
4. Xin J, Deng C, Aras O, Zhou M, Wu C, et al. 2021. Chemodynamic nanomaterials for cancer theranostics. *Journal of Nanobiotechnology* 19:192
5. Frei T, Cella F, Tedeschi F, Gutiérrez J, Stan GB, et al. 2020. Characterization and mitigation of gene expression burden in mammalian cells. *Nature Communications* 11:4641
6. Fang W, Bartel DP. 2020. microRNA clustering assists processing of suboptimal microRNA hairpins through the action of the ERH protein. *Molecular Cell* 78:289–302.e6
7. Guo T, Tang XH, Gao XY, Zhou Y, Jin B, et al. 2022. A liquid biopsy signature of circulating exosome-derived mRNAs, miRNAs and lncRNAs predict therapeutic efficacy to neoadjuvant chemotherapy in patients with advanced gastric cancer. *Molecular Cancer* 21:216
8. Zhang Q, Deng T, Zhang H, Zuo D, Zhu Q, et al. 2022. Adipocyte-derived exosomal MTTP suppresses ferroptosis and promotes chemoresistance in colorectal cancer. *Advanced Science* 9:2203357
9. Jin J, Xie Y, Zhang JS, Wang JQ, Dai SJ, et al. 2023. Sunitinib resistance in renal cell carcinoma: From molecular mechanisms to predictive biomarkers. *Resistance Updates* 67:100929
10. Li K, Chen Y, Li A, Tan C, Liu X. 2019. Exosomes play roles in sequential processes of tumor metastasis. *International Journal of Cancer* 144:1486–95
11. Jiang W, Mei WJ, Xu SY, Ling YH, Li WR, et al. 2022. Clinical actionability of triaging DNA mismatch repair deficient colorectal cancer from biopsy samples using deep learning. *eBioMedicine* 81:104120
12. Chen C, Wang J, Pan D, Wang X, Xu Y, et al. 2023. Applications of multi-omics analysis in human diseases. *MedComm(2020)* 4:e315
13. Ye Z, Yi J, Jiang X, Shi W, Xu H, et al. 2025. Gastric cancer-derived exosomal let-7 g-5p mediated by SERPINE1 promotes macrophage M2 polarization and gastric cancer progression. *Journal of Experimental & Clinical Cancer Research* 44:2
14. Piccinno E, Schirizzi A, Scalavino V, De Leonardi G, Donghia R, et al. 2024. Circulating miR-23b-3p, miR-30e-3p, and miR-205-5p as novel predictive biomarkers for ramucirumab–paclitaxel therapy outcomes in advanced gastric cancer. *International Journal of Molecular Sciences* 25:13498
15. Wang Z, Li Y, Cao J, Zhang W, Wang Q, et al. 2020. microRNA profile identifies miR-6165 could suppress gastric cancer migration and invasion by targeting STRN4. *Oncotargets and Therapy* 13:1859–69
16. Zhang J, Yu D, Ji C, Wang M, Fu M, et al. 2024. Exosomal miR-4745-5p/3911 from N2-polarized tumor-associated neutrophils promotes gastric cancer metastasis by regulating SLIT2. *Molecular Cancer* 23:198
17. Zhang Z, Pi J, Zou D, Wang X, Xu J, et al. 2019. microRNA arm-imbalance in part from complementary targets mediated decay promotes gastric cancer progression. *Nature Communications* 10:4397
18. Stevens MT, Saunders BM. 2021. Targets and regulation of microRNA-652-3p in homeostasis and disease. *Journal of Molecular Medicine* 99:755–69
19. Liu R, Zhang C, Hu Z, Li G, Wang C, et al. 2011. A five-microRNA signature identified from genome-wide serum microRNA expression profiling serves as a fingerprint for gastric cancer diagnosis. *European Journal of Cancer* 47:784–91

20. Shin VY, Ng EKO, Chan VW, Kwong A, Chu KM. 2015. A three-miRNA signature as promising non-invasive diagnostic marker for gastric cancer. *Molecular Cancer* 14:202
21. Higashijima Y, Kanki Y. 2020. Molecular mechanistic insights: The emerging role of SOXF transcription factors in tumorigenesis and development. *Seminars in Cancer Biology* 67:39–48
22. Li YZ, Mou P, Shen Y, Gao LD, Chen XX, et al. 2022. Effect of miR-184 and miR-205 on the tumorigenesis of conjunctival mucosa associated lymphoid tissue lymphoma through regulating RasL10B and TNFAIP8. *International Journal of Ophthalmology* 15:1–8
23. Feng R, Dong L. 2015. Inhibitory effect of miR-184 on the potential of proliferation and invasion in human glioma and breast cancer cells *in vitro*. *International Journal of Clinical and Experimental Pathology* 8:9376–82
24. Park JK, Peng H, Yang W, Katsnelson J, Volpert O, et al. 2017. miR-184 exhibits angiostatic properties via regulation of Akt and VEGF signaling pathways. *FASEB Journal* 31:256–65
25. Abdelbaky I, Tayara H, Chong KT. 2022. Identification of miRNA-small molecule associations by continuous feature representation using auto-encoders. *Pharmaceutics* 14:3
26. Hashimoto Y, Akiyama Y, Yuasa Y. 2013. Multiple-to-multiple relationships between microRNAs and target genes in gastric cancer. *PLoS One* 8:e62589
27. Guo J, Miao Y, Xiao B, Huan R, Jiang Z, et al. 2009. Differential expression of microRNA species in human gastric cancer versus non-tumorous tissues. *Journal of Gastroenterology and Hepatology* 24:652–57
28. Hu H, Quan G, Yang F, Du S, Ding S, et al. 2023. microRNA-96-5p is negatively regulating GPC3 in the metastasis of papillary thyroid cancer. *SAGE Open Medicine* 11:20503121231205710
29. Wang B, Liu X, Meng X. 2020. miR-96-5p enhances cell proliferation and invasion via targeted regulation of ZDHHC5 in gastric cancer. *Bioscience Reports* 40:BSR20191845
30. Zhang C, Zhang CD, Liang Y, Wu KZ, Pei JP, et al. 2020. The comprehensive upstream transcription and downstream targeting regulation network of miRNAs reveal potential diagnostic roles in gastric cancer. *Life Sciences* 253:117741
31. Zhang H, Du Y, Xin P, Man X. 2022. The LINC00852/miR-29a-3p/JARID2 axis regulates the proliferation and invasion of prostate cancer cell. *BMC Cancer* 22:1269
32. Miyake M, Hori S, Morizawa Y, Tatsumi Y, Toritsuka M, et al. 2017. Collagen type IV alpha 1 (COL4A1) and collagen type XIII alpha 1 (COL13A1) produced in cancer cells promote tumor budding at the invasion front in human urothelial carcinoma of the bladder. *Oncotarget* 8:36099–114
33. Kim HY, Kim YM, Hong S. 2019. Astaxanthin suppresses the metastasis of colon cancer by inhibiting the MYC-mediated downregulation of microRNA-29a-3p and microRNA-200a. *Scientific Reports* 9:9457
34. Xiao Y, Yang P, Xiao W, Yu Z, Li J, et al. 2025. POU2F1 inhibits miR-29b1/a cluster-mediated suppression of PIK3R1 and PIK3R3 expression to regulate gastric cancer cell invasion and migration. *Chinese Medical Journal* 138:838–50
35. Menon A, Abd-Aziz N, Khalid K, Poh CL, Naidu R. 2022. miRNA: a promising therapeutic target in cancer. *International Journal of Molecular Sciences* 23:11502
36. Xu W, Lu M, Xie S, Zhou D, Zhu M, et al. 2023. Endoplasmic reticulum stress promotes prostate cancer cells to release exosome and up-regulate PD-L1 expression via PI3K/Akt signaling pathway in macrophages. *Journal of Cancer* 14:1062–74
37. Liu CY, Zhao WL, Wang JX, Zhao XF. 2015. Cyclin-dependent kinase regulatory subunit 1 promotes cell proliferation by insulin regulation. *Cell Cycle* 14:3045–57
38. Gu J, Han T, Sun L, Yan AH, Jiang XJ. 2020. miR-552 promotes laryngocarcinoma cells proliferation and metastasis by targeting p53 pathway. *Cell Cycle* 19:1012–21



Copyright: © 2025 by the author(s). Published by Maximum Academic Press, Fayetteville, GA. This article is an open access article distributed under Creative Commons Attribution License (CC BY 4.0), visit <https://creativecommons.org/licenses/by/4.0/>.